
Optical spectroscopy and imaging of the dentin–enamel junction in human third molars

R. R. Gallagher,¹ S. G. Demos,² M. Balooch,³ G. W. Marshall, Jr.,^{1,4} S. J. Marshall^{1,4}

¹Bioengineering Graduate Group, University of California at San Francisco/University of California at Berkeley, San Francisco/Berkeley, California

²Lawrence Livermore National Laboratory, Livermore, California

³Department of Chemistry and Materials Science, Lawrence Livermore National Laboratory, Livermore, California

⁴Division of Biomaterials and Bioengineering, Department of Preventive and Restorative Dental Sciences, University of California, San Francisco, San Francisco, California

Received 12 September 2000; revised 29 October 2001; accepted 15 November 2001

Abstract: A 351-nm laser excitation source was used to perform autofluorescence microscopy of dentin, enamel, and the dentin–enamel junction (DEJ) to obtain information regarding their morphology and spectral characteristics. The emission spectra of these calcified dental tissues were different from one another, and this enabled the DEJ to be imaged and dimensionalized. The DEJ displayed sharp and clearly delineated borders at both its enamel and dentin margins. The dentinal tubules and the enamel prisms ap-

peared to terminate abruptly at the DEJ. The median DEJ width was 10 μm , ranging from 7 to 15 μm , and it did not appear to depend on intratooth position. © 2002 Wiley Periodicals, Inc. *J Biomed Mater Res* 64A: 372–377, 2003

Key words: dentin–enamel junction (DEJ); width estimate; emission spectroscopy; fluorescence spectra; biological interfacial material

INTRODUCTION

The dentin–enamel junction (DEJ) is a critical interface that joins hard, brittle enamel with tough dentin.¹ During tooth formation, the DEJ functions as the initiation surface for amelogenesis and odontogenesis, with enamel forming radially outward and dentin forming inward from this surface. The DEJ has been described as having a scalloped topography, with concavities directed toward the enamel and convexities directed toward the dentin.^{2,3} The scallops are subdivided by microscallops and a finer submicroscopic structure, forming a three-level microstructure. The geometry and composition of the DEJ are believed to enhance bonding between dentin and enamel and mitigate the effects of crack propagation between

these tissues. Little information presently exists regarding the dimensionality and variability of these structures.^{4,5}

Whittaker⁵ examined 162 deciduous and permanent teeth extracted from monkeys and humans and found considerable variability in the DEJ. Scalloping of monkey teeth was not observed, but 5- μm depressions near the ends of the enamel prisms were usually seen. In humans, Whittaker observed scallops of about 25–100 μm and noted that the proximal surfaces displayed greater scalloping than either the buccal or lingual surfaces. Scott and Symons⁶ reported increased scalloping under the cusps, whereas Schour⁷ found more scalloping in the gingival third of the tooth.

Lin³ used high-resolution scanning electron microscopy (SEM) and immunolabeling to identify the type and orientation of collagen present in human DEJ. Type I collagen fibrils were present in the scalloped and microscalloped areas. Lin reported that the collagen fibrils appeared to emanate from the dentin and coalesced to form coarse fibrils approximately 100 nm in diameter that traversed the DEJ before insertion into the enamel mineral. The scalloping was on the order of 25–40 μm . Lin postulated that the DEJ is a tough, distinct dental tissue essential to joining dentin

Correspondence to: G. W. Marshall, Jr.; e-mail: graymar@itsa.ucsf.edu

Contract grant sponsor: U. S. Department of Energy; contract grant number: W-7405-Eng-48

Contract grant sponsor: National Institutes of Health/National Institute of Dental and Craniofacial Research; contract grants numbers: R01 DE13029, K16 DE00386

and enamel that functions to prevent catastrophic tooth fracture by blunting and turning the crack and absorbing its driving energy. Lin³ and Lin and Douglas⁸ investigated the architecture, mechanical properties, and fracture toughness of bovine DEJ with SEM and conventional fracture mechanics approaches. They determined that the mechanical properties of the DEJ had a graded functional width of 50–100 μm in bovine teeth, and they reported that the functional width appeared to be greater than its optical appearance. They were unable to find any clear demarcation of the borders of the DEJ and were unable to correlate the mechanical and optical properties.

White et al.⁹ used microindentations across the DEJ from dentin to enamel to study the changes in micro-mechanical properties across the interface. They found a 100- μm -wide region in which the microhardness values decreased from enamel to dentin. They noted that this functional width appeared to be greater than the actual width of the DEJ. Elliot et al.¹⁰ performed a microradiodensity survey across the DEJ and reported a profile consistent with White et al.'s microindentation results. Common features included the graded transition from enamel to dentin, a small peak on the enamel side near the DEJ, and a dip on the dentin side.

Marshall et al.²² used nanomechanical testing and local polynomial regression fits of reduced modulus data to estimate the functional width of the DEJ at 11.8 μm . They reported that this value did not vary significantly from tooth to tooth or with intratooth location. Balooch et al.¹¹ used laser-induced fluorescence spectroscopy to study the architecture and composition of human dentin. They used a 351-nm argon-ion laser source to illuminate dry, polished samples of human third molars, and they determined emission spectra for normal and transparent dentin. They provided an initial estimate of the width of the DEJ (on the basis of fluorescence spectroscopy) of 10–20 μm .¹²

In 1911, Stubel¹³ introduced optical spectroscopy into the field of dental research when he reported the presence of tooth fluorescence under ultraviolet photoexcitation. Eisenberg¹⁴ reported the presence of tooth fluorescence under blue or violet light excitation. Alfano and Yao¹⁵ published the first systematic spectroscopic investigation comparing carious and non-carious teeth nearly 50 years later. Additional work has been conducted and published in the area that better defines the effects of dental caries.^{16–18} The use of optical spectroscopy in this field has grown to include the detection of dental caries.^{19,20}

This article represents an effort to determine the width, morphology, and fluorescence spectra of the human DEJ with optical spectroscopy techniques. A 351-nm laser source was used to determine emission spectra and emission ratios for enamel, dentin, and DEJ. The width and morphology of the DEJ were de-

termined from differences in the fluorescence characteristics of the tissue components.

MATERIALS AND METHODS

Sample preparation

Third molars were collected from research subjects requiring third molar extractions as part of their dental treatment plan. All subjects enrolled in this research responded positively to our informed consent document, which was approved by the University of California at San Francisco Institutional Committee on Human Research. After extraction, all teeth were sterilized by γ irradiation and stored in filtered and purified water at 4°C until they were prepared.⁴ Five teeth were sagittally sectioned across the center of the tooth for the preparation of 1-mm-thick slabs containing enamel, dentin, and DEJ. The surface of each slab was metallographically polished with a series of silicon carbide abrasive papers down to 4000 mesh. The samples were then successively polished with alumina powder slurries of 1, 0.3, and 0.05 μm . All samples were ultrasonically cleaned in filtered and purified water at the end of each polishing step for the removal of polishing agents and any residual smear layer. After their preparation, samples were air-dried for 24 h before optical spectroscopy imaging.

Laser-induced fluorescence microscopy

The experimental arrangement is illustrated in Figure 1 and has been described previously.¹¹ A continuous-wave

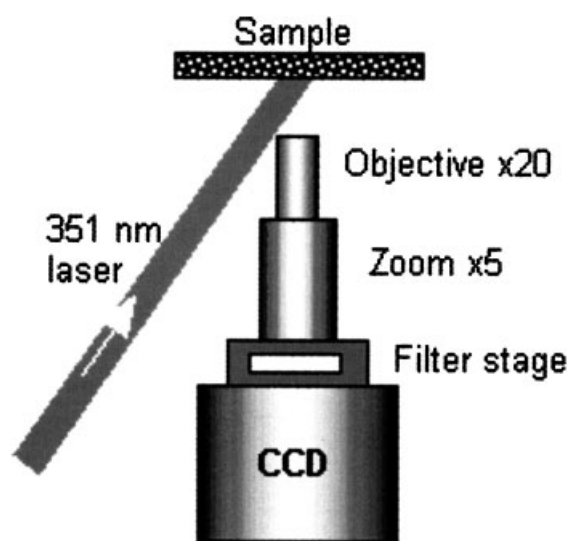


Figure 1. Autofluorescence microscopy experimental setup. A 351-nm, continuous-wave argon-ion laser was used to excite the sample. Fluoresced light was collected with a series of lenses and was passed through a filter before collection by the CCD detector.

argon-ion laser operating at 351 nm was used to excite five sagittally sectioned and polished samples from human third molars, as shown in Figure 1. The laser was oriented to strike the surface of each sample at an incident angle of approximately 45° and produced an illumination field approximately 10 mm in diameter. The intensity within the illumination field was considered to be relatively uniform. Light back-radiated from the sample was collected by a fluorescence microscope consisting of a long working-length objective lens connected in series with a 5× zoom lens. This assembly imaged the center of the illumination field and transmitted the signal to a charge coupled device (CCD) detector after passage through a narrow-pass filter. Images were captured with a liquid-nitrogen-cooled CCD detector. The spatial resolution of the system was about 1 μm. The entire apparatus was constructed on an isolation table to mitigate vibration.

Spectral construction required the use of a series of 10-nm-wide narrow-band interference filters covering the 400–850-nm range. The fluorescence microscope captured the signal return of the illuminated sample at each narrow-pass filter. All images were taken with the same perspective and magnification. In addition, each image was of the same portion of each tooth; this allowed the image data sets to be superimposed after image processing. After system calibration, spectral construction was initiated by the collection of the image data for the 400-nm narrow-pass filter. This consisted of inserting the 400-nm narrow-pass filter into the filter holder, illuminating the sample with the 351-nm argon-ion laser, and capturing the filtered and fluoresced signal with the CCD detector. After successful capture, the 400-nm filter was removed and replaced with a 410-nm filter. This sequence was continued until the 850-nm filter was reached. In this way, 45 superimposable fluorescence microscope images were recorded for each sample.

Image processing was performed after experimentation and consisted of sharpening and contrast-enhancement operations. These included pixel-by-pixel interimage processing of the digitized intensity maps, which enabled differences in the spectral characteristics of the DEJ to be distinguished from those of dentin and enamel. For accentuation of these differences, representative areas of enamel, dentin, and DEJ were identified with the displayed image intensity maps. The pixel coordinates ascribed to these tissues of interest were identified from the base image intensity map. Because the maps were superimposable, the pixel coordinates of the tissues of interest identified from the base image intensity map were used on the subsequent maps to identify the same tissue or area of interest. The intensity ascribed to the pixel coordinates of the tissue of interest at each narrow-pass filter was recorded. Spectral construction used this information collected from the 45 image intensity maps to build the spectrum for each tissue. This allowed these materials to be characterized and enabled chemical composition and mineralization changes to be studied by the comparison of their spectra.

RESULTS

Figure 2 is a fluorescence microscope image across the enamel–dentin interface of a human third molar.

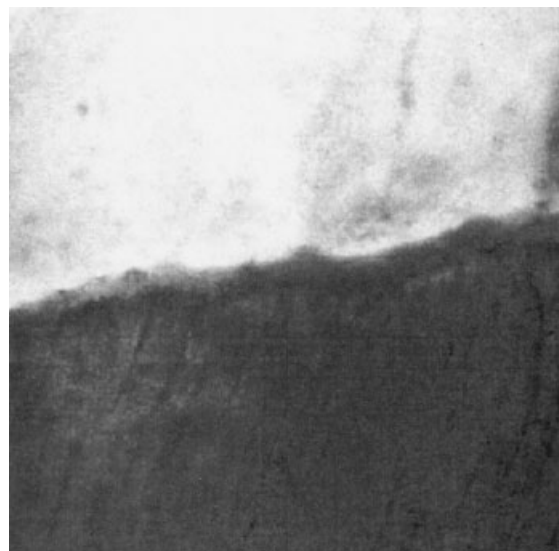


Figure 2. Fluorescence microscope image (150 μm × 150 μm) of the human DEJ. The DEJ width in this sample was estimated to be 7 μm.

The image was obtained with a 510-nm narrow-pass filter. No interimage operations were performed to increase tissue contrast on this sample. The image shows a distinct band at the interface between enamel and dentin. The dentinal tubules and enamel prisms appear to terminate on their respective sides of this band. This band displays relatively uniform emission intensity and, therefore, appears to be compositionally more homogeneous than either enamel or dentin. The width of this band, which apparently corresponds to the DEJ, was 7 μm in this sample. The width of the DEJ was measured at 10 μm with the same approach used for three other samples. The width did not appear to vary with intratooth position in any of the samples. The morphology of the DEJ in this sample and all other samples imaged appeared to follow a scalloped and subscalloped pattern.

Emission intensities from enamel, dentin, and DEJ varied from sample to sample. Because these variations may be subtle, it can be difficult for us to distinguish DEJ from enamel and dentin without resorting to image processing operations to enhance the visibility of the DEJ. An example of this condition is illustrated in Figure 3. In this image, dentin and enamel are clearly visible, but the presence of the DEJ is not readily apparent. To address this condition, we proceeded in the following manner.

Emission spectra were constructed for enamel, dentin, and DEJ as a result of 351-nm argon-ion laser excitation with the 45 superimposable fluorescence images, as described previously. Figure 4 shows the emission spectra normalized to the peak intensity and vertically translated to facilitate comparison. Enamel was broken down into either bulk or tuft. In general, spectra for enamel, dentin, and DEJ were found to be

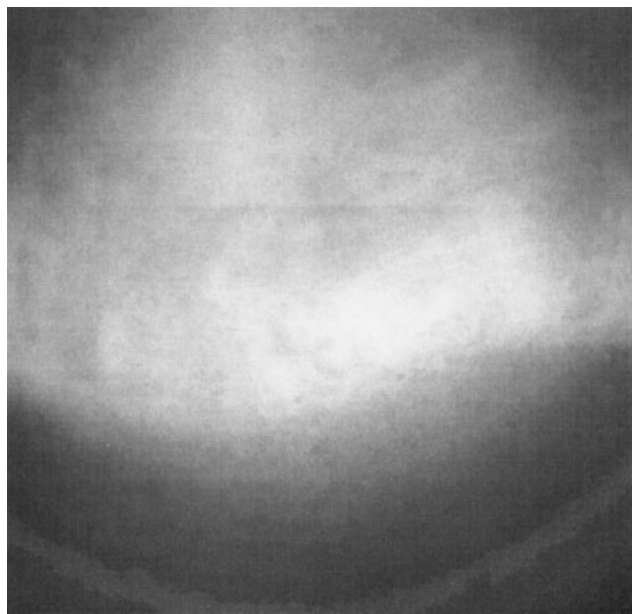


Figure 3. Fluorescence microscope image ($880\ \mu\text{m} \times 860\ \mu\text{m}$) of the human DEJ region taken with a 600-nm filter.

similar. An emission band centered at 450 nm was common to each tissue. In dentin, a second emission band is centered at 490 nm, which is consistent with previously reported emission spectra from dentin under 351-nm excitation.¹¹ Enamel showed a second emission band broader than that in dentin and located at a longer wavelength, approximately 530 nm. This is the case for both bulk and tuft enamel. For the DEJ, the second band is broad, as is that of enamel, but the peak is centered at 490 nm.

To better delineate these spectral differences, we

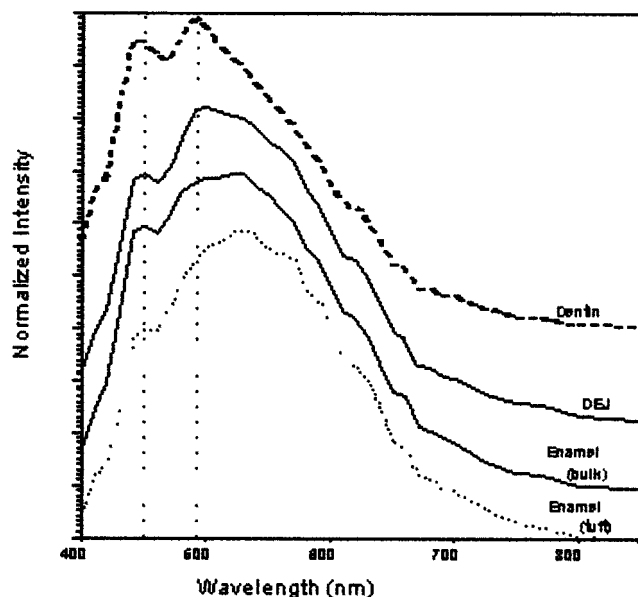


Figure 4. Tissue-specific spectra under 351-nm argon-ion excitation.

calculated emission spectrum ratios for the sample, and they are shown in Figure 5. The dentin/DEJ emission ratio suggests that dentin is relatively more emissive at shorter wavelengths than the DEJ. The enamel/DEJ emission ratio indicates that the DEJ is relatively more emissive at shorter wavelengths than enamel. Finally, the enamel/dentin emission ratio shows that enamel increases its emissivity at longer wavelengths. The results indicate that most of the relative changes in the emission spectra take place within the 400–600-nm range. To enhance the visibility of the DEJ, we used differences in the fluorescence image intensity maps. A pixel-by-pixel interimage emission spectrum ratio with the 600-nm and 410-nm image intensity maps was performed. The resulting image is shown in Figure 6. In this image, the DEJ is visible as a strip between dentin and enamel. The width of the DEJ in this sample was estimated by this method to be $15\ \mu\text{m}$. This approach also seemed to permit visualization of enamel tufts.

DISCUSSION

To date, information on the width and architecture of the DEJ has been conflicting. Various instrumentation modalities have been employed in attempts to delineate the width and morphology of the DEJ. Lin and Douglas⁸ determined that a graded functional width, on the basis of micromechanical testing of bovine teeth, existed on the order of $50\text{--}100\ \mu\text{m}$. They noted that this functional width appeared to be greater than its optical appearance. White et al.⁹ estimated the functional width of human DEJ to be $100\ \mu\text{m}$ on the

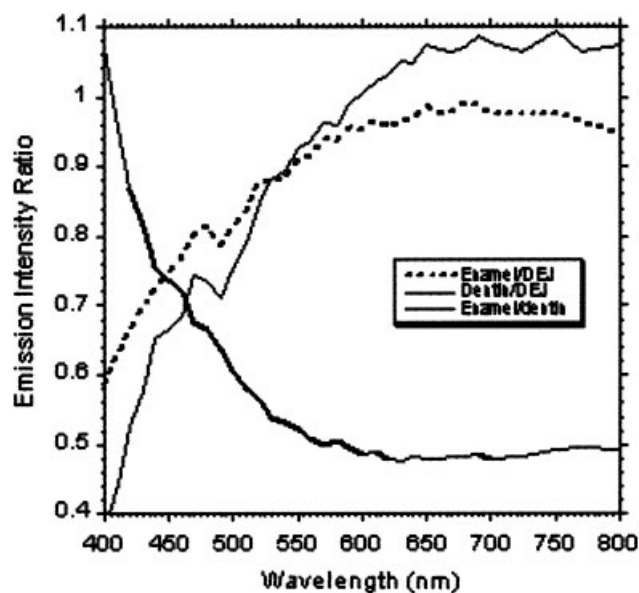


Figure 5. Emission ratios.



Figure 6. Emission ratio (600 nm/410 nm). The DEJ width in this sample was estimated to be 15 μm .

basis of microhardness testing. They noted that this width also appeared to be greater than the optical width, which they estimated as being less than 2 μm . In a preliminary study, Demos et al.¹¹ used laser-induced fluorescence spectroscopy and estimated the width of the DEJ to be 10–20 μm .

Our results indicate that the DEJ exhibits distinct and clearly defined borders with fluorescence imaging induced by a 351-nm argon-ion laser and that its median width is 10 μm . For the tooth in which the enamel, dentin, and DEJ emission intensities were similar, interimage emission ratio operations were performed to accentuate tissue contrast. This approach resulted in a DEJ width estimate of 15 μm for the specimen. The DEJ width was estimated in four specimens in which the emission intensities displayed sufficient tissue contrast differences that additional interimage operations were not performed; this resulted in width estimates ranging from 7 to 10 μm . The DEJ width was not observed to vary with intratooth position in any of the teeth tested. Our estimates of the DEJ width are much smaller than those previously reported in the literature.

In addition, we found that the emission spectra of the enamel, dentin, and DEJ as a result of 351-nm laser excitation were similar. The first emission peak of each tissue was found to be located at 450 nm. These peaks suggest that these materials have, in general, similar compositions. This is expected because they contain similar apatite phases. Differences in emission spectra were principally related to the location and character of the second peak. These differences, and differences in the emission ratios, may be explained by the compositional differences of these tissues. Dentin contains

a larger portion of organic matter than enamel, whereas enamel contains a greater amount of minerals. Although fluorescence under 351-nm excitation may be due to both organic and inorganic matter, emission from organic matter is more intense in the 400–500-nm region. This results in dentin being blue-shifted or relatively more emissive than enamel at lower wavelengths. The second peak of dentin is narrow and located at 490 nm. However, enamel exhibits a stronger emission at longer wavelengths that may be attributed to the emission characteristics of the mineral fraction. This results in a broadening of the second spectral band and a redshift of the second peak to 530 nm. This is consistent with the experimental results of Emami et al.²¹ and indicates that mineral loss in enamel is accompanied by lower fluorescence emission intensity, as measured by a yellow high-pass filter (above the 520-nm spectral region).

The emission spectrum of the DEJ contains a broad second emission band that extends toward longer wavelengths and is similar in character to that seen in enamel. This suggests that the DEJ contains a significant mineral fraction. The second peak is positioned at 490 nm, the same second peak location exhibited by dentin. This suggests that the DEJ is also composed of a large amount of organics, like dentin, and that the organics are responsible for the position of the second emission peak at 490 nm. Other analytical techniques may be required to clarify this point.

CONCLUSIONS

Laser-induced autofluorescence or emission spectroscopy can be used to characterize enamel, dentin, and the DEJ. With this technique, the DEJ was found to be a tissue spectroscopically distinct from either enamel or dentin. This property was exploited with microscopic fluorescence imaging, which allowed for the delineation of the margins of the different tissue types. The width of the DEJ was estimated to be 7–15 μm , with a median width estimate of 10 μm . The DEJ width was independent of intratooth position. The first emission peaks of dentin, enamel, and the DEJ were located at 450 nm. The second peaks of dentin and the DEJ were located at 490 nm. These peaks were narrow for dentin and broad for DEJ. Enamel exhibited a broad second peak at 530 nm.

The emission spectroscopy results suggest that the DEJ is composed of large amounts of organic and mineral matter and that the width is usually well defined and uniform under excitation by a 351-nm argon-ion laser. Future instrumentation with other analytical methods could be used to improve our understanding of the composition of the DEJ.

This work was performed at Lawrence Livermore Na-

tional Laboratory under the auspices of the U.S. Department of Energy through the Institute for Laser Science and Applications and was supported by the U. S. Public Health Service through National Institutes of Health/National Institute of Dental and Craniofacial Research grants to R. R. Gallagher and G. W. Marshall, Jr.

References

1. Marshall GW. Dentin: Microstructure and characterization. *Quintessence Int* 1993;24:606-617.
2. Bhaskar SN, editor. *Orban's oral histology and embryology*. Chicago: Mosby; 1990.
3. Lin CP. Structure-function property relationships in the dentin-enamel complex and tooth restoration interface [PhD thesis]. University of Minnesota, Minneapolis, MN; 1993.
4. White JM, Goodis HE, Marshall SJ, Marshall GW. Sterilization of teeth by gamma radiation. *J Dent Res* 1984;73:1560-1567.
5. Whittaker DK. The enamel-dentine junction of human and Macaca Iru teeth: A light and electron microscopic study. *J Anat* 1978;125:323-335.
6. Scott JH, Symons NBB. *Introduction to dental anatomy*. Edinburgh: Churchill Livingstone; 1971.
7. Schour I. *Noyes oral histology and embryology*. London: Kimpton; 1960.
8. Lin CP, Douglas WH. Structure-property relations and crack resistance at the bovine dentin-enamel junction. *J Dent Res* 1994;73:1072-1078.
9. White SN, Paine ML, Luo W, Sarikaya M, Fong H, Yu A, Li ZC, Snead ML. The dentin-enamel junction is a broad transitional zone uniting dissimilar bioceramic composites. *J Am Ceram Soc* 2000;83:238-240.
10. Elliot JC, Anderson P, Gao XJ, Wong FSL, Davis GR, Dowker SEP. Application of scanning microradiography and X-ray microtomography to studies of teeth and bone. *J X-Ray Sci Technol* 1994;4:102-117.
11. Balooch M, Demos SG, Kinney JH, Marshall GW, Balooch G, Marshall SJ. Local mechanical and optical properties of healthy and transparent root dentin. *J Mater Sci Mater Med* 2001;12: 507-514.
12. Demos SG, Balooch M, Marshall GW, Marshall SJ, Gallagher RR. Optical spectroscopy of transparent non-cariou human dentin and dentin-enamel junction. In: Featherstone JD, Rechmann P, Fried D, editors. *Lasers in dentistry*. Bellingham, WA: SPIE—The International Society for Optical Engineering; 1999. Vol. 6, p 102-105.
13. Stubel H. Die fluoreszenz tierische gewebe in ultra-violettem licht. *Pflingers Arch Ges Physiol* 1911;141:1.
14. Eisenberg J. Phenomena observed by subjecting dental tissues to ultra-violet rays corresponding to approximately 3590AU. *Dent Cosmos* 1933;5:284.
15. Alfano RR, Yao SS. Human teeth with and without dental caries studied by visible luminescent spectroscopy. *J Dent Res* 1981;54:67.
16. Bjelkhagen H, Sundstrom F, Angmar-Manson B, Ryden H. Early detection of enamel caries by luminescence excited by visible laser light. *Swed Dent J* 1982;6:1.
17. Alfano RR, Yao SS. Human teeth with and without dental caries studied by laser scattering, fluorescence and absorption spectroscopy. *IEEE J Quantum Electron* 1984;20:1512.
18. Sundstrom F, Fredriksson K, Montan S, Hafstrom-Bjorkman U, Strom J. Laser induced fluorescence from sound and carious tooth substance: Spectroscopic studies. *Swed Dent J* 1985;9:71.
19. Lussi A, Imwinkelried S, Pitts NB, Longbottom C, Reich E. Performance and reproducibility of a laser fluorescence system for detection of occlusal caries in vitro. *Caries Res* 1999;33:261.
20. Hibst R, Paulus R. Caries detection by red excited fluorescence: investigations of fluorophores. *Caries Res* 1999;33:295.
21. Emami Z, Al-Khateeb S, de Josselin de Jong E, Sundstrom F, Trollsas K, Angmar-Mansson B. Mineral loss in incipient caries lesions quantified with laser fluorescence and longitudinal microradiography. *Acta Odontol Scand* 1996;54:8.
22. Marshall GW, Balooch M, Gallagher RR, Gansky SA, Marshall SJ. Mechanical properties of the dentinoenamel junction: AFM studies of nanohardness, elastic modulus, and fracture. *J Biomed Mater Res* 2001;54:87-95.